Variational cluster approach to the Hubbard model: Phase-separation tendency and finite-size effects

M. Aichhorn,[1] E. Arrigoni,[2] M. Potthoff,[1,3] and W. Hanke[1]
[1]*Institute for Theoretical Physics, University of Würzburg, Am Hubland, 97074 Würzburg, Germany*
[2]*Institute of Theoretical Physics and Computational Physics, Graz University of Technology, Petersgasse 16, 8010 Graz, Austria*
[3]*Institute for Theoretical Physics, University of Leipzig, vor dem Hospitaltore 1, 04103 Leipzig, Germany*
(Received 11 September 2006; published 22 December 2006)

Using the variational cluster approach, we study the transition from the antiferromagnetic to the superconducting phase of the two-dimensional Hubbard model at zero temperature. Our calculations are based on a method to evaluate the VCA grand potential which employs a modified Lanczos algorithm and avoids integrations over the real or imaginary frequency axis. Thereby, very accurate results are possible for cluster sizes not accessible to full diagonalization. This is important for an improved treatment of short-range correlations, including correlations between Cooper pairs in particular. We apply this improved method in order to investigate the cluster-size dependence of the phase-separation tendency that has been proposed recently on the basis of calculations for smaller clusters. While the energy barrier associated with phase separation rapidly decreases with increasing cluster size for both hole and electron doping, the extension of the phase-separation region behaves differently in the two cases. More specifically, our results suggest that phase separation remains persistent in the hole-doped case and disappears in the electron-doped case. We also study the evolution of the single-particle spectrum as a function of doping and point out the relevance of our results for experimental findings in electron and hole-doped materials.

DOI: 10.1103/PhysRevB.74.235117 PACS number(s): 71.10.−w, 74.20.−z, 75.10.−b, 71.30.+h

I. INTRODUCTION

Since the discovery of high-temperature superconductivity in copper-based transition-metal oxides, a tremendous effort has been devoted to establish a convincing theory that covers the general aspects of their unusual and fascinating physics. The attempts are complicated by the fact that strong electron correlations play a key role in the physics of the cuprates. A central question in this context concerns the emergence of small energy scales, much smaller than the bare (Coulomb) interactions between the electrons, which govern the existence and the competition of different phases at low temperatures. This can be studied by considering prototypical lattice models of strongly correlated electrons. Some agreement has been achieved that the relevant physics of the cuprate high-temperature superconductors is covered by the two-dimensional one-band Hubbard model (Ref. 1)

$$H = \sum_{i,j,\sigma} t_{ij} c^{\dagger}_{i\sigma} c_{j\sigma} + U \sum_{i} n_{i\uparrow} n_{i\downarrow} - \mu \sum_{i} n_{i}. \qquad (1)$$

Here t_{ij} denote the hopping matrix elements, $n_{i\uparrow}$ is the density at site i with spin "↑", $n_i = n_{i\uparrow} + n_{i\downarrow}$, μ the chemical potential, and U the local Coulomb repulsion.

In recent years there has been substantial progress in the understanding of the ground-state properties of the Hubbard model due to the development of quantum-cluster theories,[2] such as cluster extensions of the dynamical mean-field theory (DMFT), i.e., the dynamical cluster approximation[3] and the cellular DMFT,[4,5] or the variational cluster approach (VCA).[6,7] These cluster calculations confirm the fact that the ground state away from half-filling has a nonvanishing superconducting order parameter[8,9,11–13] with a pairing interaction of predominantly d-wave character.[14] Recent VCA calculations[8,9,12] suggest that at low electron and hole doping the two-dimensional Hubbard model is in a symmetry-broken mixed AF+SC state where both the antiferromagnetic (AF) and the superconducting (SC) order parameters are finite. This is consistent with recent cellular DMFT calculations.[13] When going to higher dopings, the system displays a tendency to phase separate into an AF+SC phase at lower doping and a pure SC phase at higher doping.

The VCA accesses the physics of a lattice model in the thermodynamic limit by optimizing trial self-energies generated by a reference system. The above-mentioned VCA calculations are based on a reference system consisting of small (2×2) isolated clusters tiling the infinite lattice. This generates trial self-energies which are very short ranged spatially. Hence, there is the obvious question for the robustness of the results as a function of the size of the individual clusters. Up to now, it was not possible to consider larger cluster sizes and, at the same time, reach a sufficient accuracy to resolve the tiny energy scale driving phase separation, especially in the electron-doped case. The reason is that an accurate evaluation of the VCA grand potential has required a *full* diagonalization of the cluster Hamiltonian (see Ref. 9 for details) which has severely restricted the available cluster sizes.

The purpose of this paper is to present a method for the evaluation of the VCA grand potential based on the Lanczos method which leads to sufficiently accurate results even for larger clusters where full diagonalization is no longer possible. Using this method we investigate the competing phases in the two-dimensional Hubbard model at zero temperature for clusters up to ten sites. This implies a substantial qualitative step forward as short-range correlations between different Cooper pairs can be included—opposed to calculations based on 2×2 clusters.

II. VARIATIONAL CLUSTER APPROACH

The variational cluster approach is one of the possible approximation schemes that can be constructed within the self-energy-functional theory (SFT).[15] The SFT provides a variational scheme to use dynamical information from an exactly solvable "reference system" (for example an isolated cluster) to approximate the physics of a system in the thermodynamic limit. For a system with Hamiltonian $H=H_0(\boldsymbol{t})+H_1(\boldsymbol{U})$ and one-particle and interaction parameters $\boldsymbol{t}$ and $\boldsymbol{U}$, the grand potential is written as a functional of the self-energy $\boldsymbol{\Sigma}$ as follows:

$$\Omega[\boldsymbol{\Sigma}] = F[\boldsymbol{\Sigma}] + \mathrm{Tr}\,\ln(\boldsymbol{G}_0^{-1} - \boldsymbol{\Sigma})^{-1}, \tag{2}$$

with the stationary property $\delta\Omega[\boldsymbol{\Sigma}_{\mathrm{phys}}]=0$ for the physical self-energy. Here, $\boldsymbol{G}_0=(\omega+\mu-\boldsymbol{t})^{-1}$ is the free Green's function of the original model in the thermodynamic limit at frequency ω, and $F[\boldsymbol{\Sigma}]$ is the Legendre transform of the universal Luttinger-Ward functional. Due to its universality it is the same as the functional for a "simpler" problem with the same interaction but a modified one-particle part $\boldsymbol{t}'$. The stationary solutions are obtained *within* the subspace of self-energies $\boldsymbol{\Sigma}=\boldsymbol{\Sigma}(\boldsymbol{t}')$ of the simpler problem that is spanned by varying $\boldsymbol{t}'$. This restriction constitutes the approximation. Details of the approach are described in Refs. 15 and 16.

The VCA (Ref. 6) is generated within the SFT by choosing as a reference system a set of isolated clusters which tile up the original infinite lattice. By construction, the VCA correctly incorporates correlation effects in the electron self-energy up to the length scale given by the cluster size. Beyond this scale it acts like a mean-field approximation. One of the main advantages of the VCA, as compared to the simpler cluster perturbation theory,[17] consists in its ability to describe (normal and off-diagonal) long-range order by including suitably chosen fictitious symmetry-breaking Weiss fields in the set of variational parameters. Microscopically coexisting phases can be obtained using several Weiss fields. The method links in a consistent way the static thermodynamics with the frequency-dependent one-particle excitation spectra (photoemission). Details of the approach have been described elsewhere.[7–9]

The VCA grand potential to be calculated in practice reads

$$\Omega = \Omega' + \mathrm{Tr}\,\ln(\boldsymbol{G}_0^{-1} - \boldsymbol{\Sigma})^{-1} - \mathrm{Tr}\,\ln(\boldsymbol{G}'). \tag{3}$$

Here, $\boldsymbol{G}_0$ is the free Green's function of the model given by Eq. (1), Ω', $\boldsymbol{\Sigma}$, and $\boldsymbol{G}'$ are the grand potential, the self-energy, and the Green's function of the cluster reference system which depend on the one-particle parameters $\boldsymbol{t}'$. In the present study we consider clusters with $L_c=4$, 8, and 10 sites to search for the stationary solution characterized by the condition $\partial\Omega/\partial\boldsymbol{t}'=0$.[10] This stationary point provides a good approximation to the exact solution for the system in the thermodynamical limit if the self-energy is sufficiently "short ranged," i.e., sufficiently localized within the cluster.

As discussed in Refs. 8 and 9, it is important to evaluate Ω with high accuracy in order to resolve the relevant energy scales of the competing phases, especially in the electron-doped case. Here, we present a method in which this evaluation can be done without a numerical integration over frequencies [note that frequency integration is implicit in the $\mathrm{Tr}\,\ln\cdots$ terms in Eq. (3)]. We start from the expression derived in Ref. 15 which expresses the $\mathrm{Tr}\,\ln\cdots$ terms as a sum over the single-particle excitation energies:

$$\mathrm{Tr}\,\ln(\boldsymbol{G}_0^{-1} - \boldsymbol{\Sigma})^{-1} = -\sum_m T\ln(1+e^{-\beta\omega_m}) - R \overset{T=0}{=} \sum_m \omega_m\Theta(-\omega_m) - R \tag{4}$$

and

$$\mathrm{Tr}\,\ln \boldsymbol{G}' = -\sum_m T\ln(1+e^{-\beta\omega'_m}) - R \overset{T=0}{=} \sum_m \omega'_m\Theta(-\omega'_m) - R. \tag{5}$$

Here $\Theta(\omega)$ is the Heaviside step function, $\beta=1/T$ the inverse temperature. ω'_m are the one-particle excitation energies of the reference system, i.e., the poles of $\boldsymbol{G}'$, and ω_m are the poles of the VCA Green's function $(\boldsymbol{G}_0^{-1}-\boldsymbol{\Sigma})^{-1}$. R represents a contribution due to the poles of the self-energy (see Ref. 15) which cancels out in Eq. (3) and can thus be ignored. The excitation energies $\omega'_m=E_r-E_s$ of the reference system (i.e., of the cluster) can be readily obtained with the help of the Lanczos algorithm from the eigenenergies E_r of the reference system. Here, we introduce the notation $m=(r,s)$, to indicate an excitation between two states s and r. The major difficulty consists in finding the poles ω_m of the VCA Green's function.

This can be done in the following way: Consider the Lehmann representation[18] of $\boldsymbol{G}'$ which can be cast into the form (Ref. 19)

$$G'_{\alpha\beta}(\omega) = \sum_m Q_{\alpha m}\frac{1}{\omega-\omega'_m}Q^\dagger_{m\beta}, \tag{6}$$

where α refers to the one-particle orbitals of the cluster [typically $\alpha=(\text{site } i, \text{spin } \sigma)$ but it can also include an orbital index]. The "Q-matrix" is defined:

$$Q_{\alpha m} = \langle r|c_\alpha|s\rangle\sqrt{\frac{\exp(-\beta E_r)+\exp(-\beta E_s)}{Z'}} \overset{T=0}{=} \delta_{r,0}\langle 0|c_\alpha|s\rangle + \delta_{s,0}\langle r|c_\alpha|0\rangle. \tag{7}$$

The spectral weight (residue) of $G'_{\alpha\beta}(\omega)$ at a pole $\omega=\omega'_m$ is given by $Q_{\alpha m}Q^\dagger_{m\beta}$. $Z'=\Sigma_r e^{-\beta E_r}$ is the grand-canonical partition function at finite temperature, and $|0\rangle$ denotes the (grand-canonical) ground state of the reference system. Introducing the diagonal matrix $g_{mn}(\omega)=\delta_{mn}/(\omega-\omega'_m)$, we have:

$$\boldsymbol{G}'(\omega) = \boldsymbol{Q}\boldsymbol{g}(\omega)\boldsymbol{Q}^\dagger. \tag{8}$$

Defining $\boldsymbol{V}=\boldsymbol{t}-\boldsymbol{t}'$, which in case of the VCA typically includes the intercluster hopping terms, the "subtraction" of the fictitious Weiss fields, as well as shifts of the one-particle energies (see below),[9] the VCA expression for the lattice Green's function can be written:

$$\boldsymbol{G} \equiv \frac{1}{\boldsymbol{G}_0^{-1} - \boldsymbol{\Sigma}} = \frac{1}{(\boldsymbol{G}')^{-1} - \boldsymbol{V}}. \tag{9}$$

This expression can be transformed with the help of the $\boldsymbol{Q}$-matrix Eq. (7) and Eq. (8):

$$\boldsymbol{G} = \frac{1}{(\boldsymbol{Q}\boldsymbol{g}\boldsymbol{Q}^\dagger)^{-1} - \boldsymbol{V}} = \boldsymbol{Q}\boldsymbol{g}\boldsymbol{Q}^\dagger + \boldsymbol{Q}\boldsymbol{g}\boldsymbol{Q}^\dagger \cdot \boldsymbol{V} \cdot \boldsymbol{Q}\boldsymbol{g}\boldsymbol{Q}^\dagger + \cdots$$

$$= \boldsymbol{Q}(\boldsymbol{g} + \boldsymbol{g} \cdot \boldsymbol{Q}^\dagger \boldsymbol{V}\boldsymbol{Q} \cdot \boldsymbol{g} + \cdots)\boldsymbol{Q}^\dagger = \boldsymbol{Q}\frac{1}{\boldsymbol{g}^{-1} - \boldsymbol{Q}^\dagger \boldsymbol{V}\boldsymbol{Q}}\boldsymbol{Q}^\dagger. \tag{10}$$

Note that $\boldsymbol{Q}$ is not a square matrix and that $\boldsymbol{Q}\boldsymbol{Q}^\dagger = \mathbf{1} \neq \boldsymbol{Q}^\dagger\boldsymbol{Q}$. Since $\boldsymbol{g}^{-1} = \omega - \boldsymbol{\Lambda}$ with $\Lambda_{mn} = \delta_{mn}\omega'_m$, the poles of $\boldsymbol{G}$ are now simply given by the eigenvalues of the (frequency independent) matrix $\boldsymbol{M} = \boldsymbol{\Lambda} + \boldsymbol{Q}^\dagger \boldsymbol{V}\boldsymbol{Q}$ and can be easily found by diagonalization. The dimension of $\boldsymbol{M}$ is given by the number of poles of $\boldsymbol{G}'$ with nonvanishing spectral weight.[20] Hence, the above scheme requires the knowledge of all excited states of the reference system. In Refs. 8 and 9, these states have been obtained by a *full* diagonalization of a rather small (2×2) cluster.

For larger clusters, where a full diagonalization is not possible, the Lanczos algorithm should, in principle, provide precisely the required poles and matrix elements Eq. (7). In practice, however, there are some difficulties, as we discuss below. Within the Lanczos method the matrix elements $G_{\alpha\beta}(\omega) = \langle\langle c_\alpha; c_\beta^\dagger \rangle\rangle_\omega$ of a cluster Green's function at $T=0$ are determined in $2L_c$ separate Lanczos procedures.[21] In each procedure, one takes as a Lanczos initial vector one element of the sets $\{c_{1,\sigma}^\dagger|0\rangle, \ldots, c_{L_c,\sigma}^\dagger|0\rangle\}$, $\{c_{1,\sigma}^\dagger|0\rangle, \ldots, c_{L_c,\sigma}^\dagger|0\rangle\}$ where $|0\rangle$ is the cluster ground state. In principle the poles should be the same for all matrix elements of the Green's function. In practice, however, the poles obtained by the $2L_c$ runs are slightly different from each other due to the limited numerical accuracy of the Lanczos method. Therefore, this kind of Lanczos algorithm is not suited for the Q-matrix evaluation of the grand potential described above, since merging all matrix elements of $\boldsymbol{G}'$ into the compact form Eq. (8) would results in a too large matrix $\boldsymbol{M}$ that cannot be diagonalized.

Fortunately, the problem can be overcome by means of the so-called *band Lanczos* method.[22] The difference with respect to the standard algorithm is that the sets of initial vectors given above are used *simultaneously* within *one single* Lanczos run. This yields the same set of poles for all index pairs (α, β) as well as the corresponding weights. The dimension of the matrix $\boldsymbol{M}$ is given by the number of iteration steps $2S_L$ in the Lanczos procedure. In this case, one only needs two Lanczos procedures instead of $2L_c$. Using this method, one introduces an error due to the limited set $(2S_L)$ of the excited states in the reference system that are kept in the Lanczos calculation. Generally, however, this error is extremely small since excitations with large weight result from states which converge very fast with increasing S_L. These excitations with large weight, on the other hand, are just those which are dominant in Eq. (3) compared to excitations with small weight.[15]

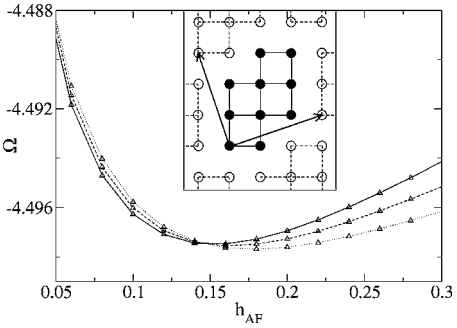

FIG. 1. The SFT grand potential Ω of the half-filled $(n=1)$ Hubbard model with nearest-neighbor hopping $t=-1$ and $U=8t$ as a function of the variational parameter h_{AF} (staggered magnetic Weiss field). Reference system (inset): $L_c=10$ clusters. We compare results obtained by integration over real frequencies with Lorentzian broadenings $\eta=0.1$ (dotted lines) and $\eta=0.05$ (dashed lines), as well as for the Q-matrix evaluation (see text, solid lines). $S_L=100$ Lanczos iteration steps have been performed.

We have checked the accuracy of our method by considering the symmetry-broken antiferromagnetic phase of the Hubbard model at half-filling (Fig. 1). One can clearly see that the Q-matrix evaluation perfectly gives the extrapolation of results obtained by numerical frequency integration with finite but small Lorentzian broadenings η. We also verified that the results converge very fast with S_L, i.e., typically $S_L \approx 100$ is fully sufficient. Last but not least, this improved method substantially reduces the computational time. For example, a factor of approximately 15 is gained for the $L_c = 10$ cluster.

III. RESULTS FOR COMPETING PHASES

On the basis of this improved evaluation, we investigate the finite-size behavior of the phase-separation tendency observed for small clusters in Ref. 8. As variational parameters we use the Weiss fields h_{AF} and h_{SC} to allow for antiferromagnetic (AF) and d-wave superconducting (SC) orders, respectively,[7,8] as well as an overall shift ε of the one-particle energies in the cluster to ensure a consistent treatment of the particle density.[9] Figure 2 shows our results for the two-dimensional Hubbard model with $U=8t$ and next-nearest-neighbor hopping $t'=-0.3t$ for the case of hole doping. The calculations have been performed for $L_c=4$ (top), $L_c=8$ (middle), and $L_c=10$ clusters (bottom).

We consider the case of hole-doping first. One can immediately see that the phase-separation tendency, found for the $L_c=4$ cluster, weakens progressively when increasing the cluster size. In particular, the corresponding "energy scale" $\Delta\mu = \mu^* - \mu_c$ diminishes very rapidly with increasing L_c ($\Delta\mu=0.050$ for $L_c=4$, $\Delta\mu=0.027$ for $L_c=8$, and $\Delta\mu=0.003$ for $L_c=10$), and appears to vanish in the $L_c \to \infty$ limit. Here, μ^* is the point where the slope of $\mu(x)$ changes sign and μ_c the chemical potential at the transition point. However, this fact does not necessarily imply the absence of macroscopic phase separation in the exact ground state of the model under study. As a matter of fact, the exact function $\mu(x)$ *must* have a nonpositive slope. Therefore, in the phase-separated case

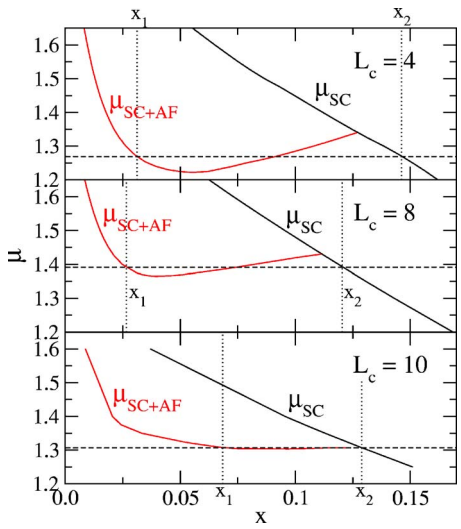

FIG. 2. (Color online) Chemical potential μ as function of hole doping x. Results for $L_c=4$ (2×2), $L_c=8$ (4×2), and $L_c=10$ clusters. The horizontal dashed lines mark the critical μ_c, and the vertical dotted lines mark the boundaries x_1 and x_2 of the phase separation region in between.

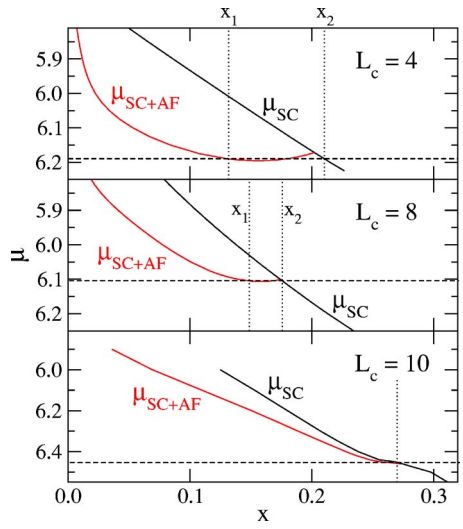

FIG. 3. (Color online) Same as Fig. 2 but for electron doping. Note that there is no phase separation for $L_c=10$; the dotted line marks the quantum critical point.

$\mu(x)$ becomes a straight line between the two boundaries of the phase-separation region x_1 and x_2.[24] Whether the exact ground state supports phase separation can be derived from the finite-size scaling of the doping discontinuity $\Delta x \equiv x_2 - x_1$, see Table I. Unfortunately, no regular finite-size behavior can be inferred from Fig. 2 and Table I for hole doping, probably due to the fact that the clusters are still too small. Opposed to the clear trend visible for the electron-doped case (see Table I), there is a much weaker L_c dependence of the discontinuities Δx, ΔM, and ΔD, which we rather interpret as being irregular. However, our results do not exclude microscopic phase separation to persist for $L_c\to\infty$. The inclusion of long-range Coulomb interaction would then be necessary in order to "frustrate" the phase separation occurring in the plain Hubbard model and produce microscopic inhomogeneous phases, such as stripes.[23,27,28] We stress that at this point only qualitative estimates for $L_c\to\infty$ rather than a convincing finite-size scaling are possible. For a discussion on these issues see, e.g., Refs. 24–26.

The situation is quite different in the electron-doped case (see Fig. 3). Here, not only the phase-separation energy $\Delta\mu$, but also the doping discontinuity Δx appears to vanish for $L_c\to\infty$. In fact, $\Delta\mu$ is already an order of magnitude smaller than for hole doping in the $L_c=4$ cluster.[8] In addition, already for $L_c=10$ the transition from the AF+SC to the pure SC phase has become continuous at least within numerical accuracy. In this case, the weak phase separation observed at the mean-field level for small clusters was simply a signal of a *tendency* of the system to produce *microscopically* inhomogeneous phases (such as stripes), as conjectured in Ref. 8. The fact that the corresponding energy scale is already very small for a small cluster could explain why there is no clear sign of stripes in electron-doped materials and could possibly be related to the much smaller pseudogap energy scale, as discussed in Refs. 8 and 9.

TABLE I. Discontinuities Δx, ΔM, and ΔD across the PS region for hole and electron doping.

h-Doping	Δx	ΔM	ΔD
$L_c=4$	0.115	0.717	0.055
$L_c=8$	0.094	0.699	0.043
$L_c=10$	0.056	0.568	0.032
e-Doping	Δx	ΔM	ΔD
$L_c=4$	0.079	0.476	0.016
$L_c=8$	0.020	0.316	0.004
$L_c=10$	0.000	0.000	0.000

Contrary to the phase-separation energy, the AF and SC order parameters M and D plotted in Fig. 4 only display a rather weak cluster-size dependence. This shows that already a small 2×2 cluster describes the static ground-state quan-

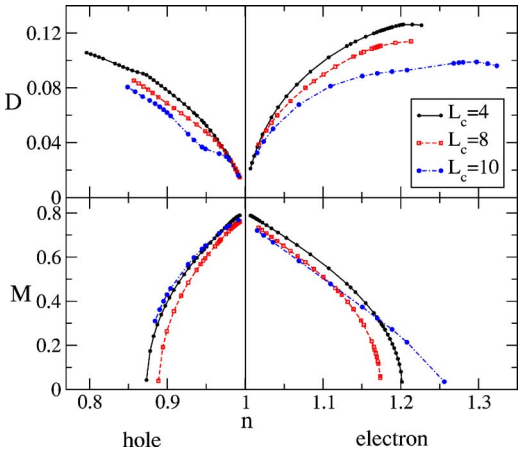

FIG. 4. (Color online) Magnetization M and d-wave order parameter D as functions of hole and electron doping for $L_c=4$, 8, and 10.

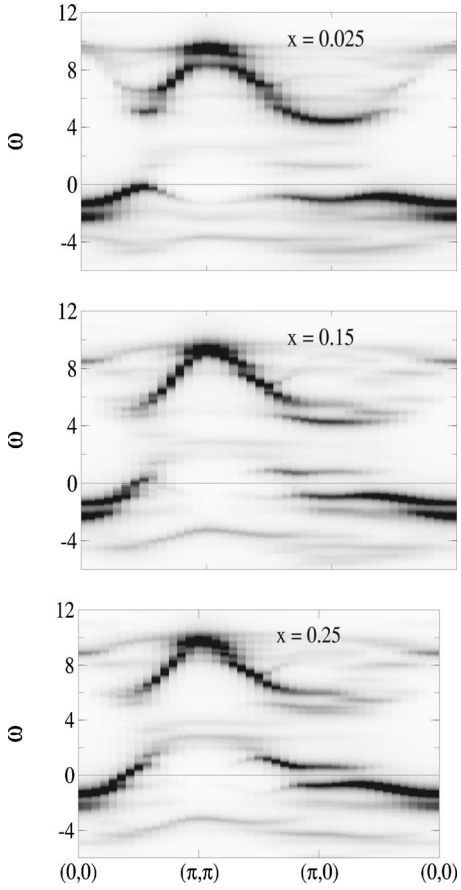

FIG. 5. Evolution of the spectral function upon hole doping ($L_c=8$). Top panel: doping $x=0.025$, mixed SC+AF phase. Middle panel: $x=0.15$, SC phase. Bottom panel: $x=0.25$, SC phase. A Lorentzian broadening of $\eta=0.2t$ has been used to display the results.

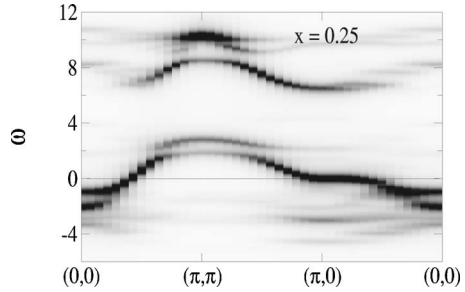

FIG. 6. Spectral function for $x=0.25$ ($L_c=8$), SC phase, as in Fig. 5 but for a different stationary point with a particle density $n'=0.75\cdots$ in the cluster.

ties with a rather good accuracy, except for cases close to a phase transition. Finite-size effects are more pronounced for D because the SC order parameter is a nonlocal quantity which converges slower with increasing cluster size as compared to M. Nevertheless, from our results we can argue that for both, hole and electron doping, at least substantial SC fluctuations remain in the thermodynamic limit even in the AF phase. A more precise finite-size scaling to identify as to whether one really has long-range SC order is not possible since that would involve larger constant cluster shapes ($2\times2, 4\times4,\ldots$) which are not accessible by the present VCA.

The comparison of Fig. 4 with previous calculations[12] shows that the inclusion of the energy shift ε as a variational parameter provides results which depend only weakly on the cluster size L_c. For example, we find a mixed AF+SC phase for small doping for all cluster sizes considered. This can be understood by the fact that the inclusion of additional variational parameters "optimize" the ground state of the reference system toward the exact solution of the infinite lattice.

Figure 5 shows the evolution of the single-particle spectral function upon hole doping calculated with the $L_c=8$ reference system. In the upper plot for doping $x=0.025$, the system is still in the mixed AF+SC phase. This is the reason for the "back-turning" of the quasi-particle-like band around $(\pi/2,\pi/2)$ although the chemical potential already "touches" the band at this wave vector. For higher doping (middle and lower panel), we clearly see a transition to a dispersion crossing the chemical potential in the nodal direction, in agreement with angle-resolved photoemission experiments. The low-energy coherent quasiparticle band with a width of the order of a few times J has been replaced by a band of width of a few times t. The qualitative trend is well known from QMC calculations.[30] This represents a clear improvement as compared to our previous results for $L_c=4$ clusters, where the dispersion in the nodal direction showed back-turning signals also for higher dopings.

In spite of the improvement for the nodal direction, the d-wave SC gap appears to be too large for the slightly overdoped case $x=0.25$. Furthermore, for higher dopings one expects a decrease of the weight of the upper Hubbard band which is much stronger than visible in the $x=0.25$ spectrum. The reason for these shortcomings is probably too strong an admixture of the half-filled cluster ground state: In the absence of superconductivity and for not too high doping, the particle density of the reference system (the isolated cluster) is $n'=1$. In our case, deviations from cluster half-filling are introduced due to a nonvanishing SC Weiss field only. For $L_c=8$ we find $n'=0.92$ at $x=0.25$ which is still close to half-filling.

A physically better description of the spectral density at higher dopings can only be achieved when (in the absence of superconductivity) starting from a cluster ground state with $n'<1$. This yields a corresponding SFT grand potential which has to be compared with the SFT grand potential for the $n'=1$ stationary point. Note that for a vanishing SC Weiss field, the VCA cannot give a grand potential that is continuous in the entire doping range. This is an artifact of the VCA which levels off and eventually becomes irrelevant in the large-cluster limit.

In fact, there is a second stationary point for $x=0.250$ with a particle density in the cluster $n'=0.755$. Due to the nonvanishing SC Weiss field, this is close but not equal to the commensurate cluster filling $n'=0.75$. This stationary point, however, exhibits an SFT grand potential which is *higher* as compared to that of the $n'=0.92$ solution and, consequently, should be disregarded. It is nevertheless interesting to discuss the spectral density of this (metastable) state which is shown in Fig. 6. As could have been expected, the SC gap is much smaller (and actually not visible on the scale of the

figure) and, as compared to the corresponding spectrum in Fig. 5, the weight of the upper Hubbard band is clearly reduced. Moreover, signatures of magnetic order are no longer visible in this spectrum.

IV. CONCLUSIONS

We have developed a method to evaluate the VCA grand potential which avoids numerical integrations over real or Matsubara frequencies, even for large clusters, for which a complete diagonalization is not feasible. This provides a sufficient accuracy to study the cluster-size dependence of the phase-separation tendency obtained in previous works. The results of the present paper suggest that in the hole-doped case phase separation observed for small clusters persists for $L_c \to \infty$, i.e., in the exact ground state, while it eventually disappears in case of electron doping. This would explain why there is no clear sign of stripes in electron-doped materials, and could possibly be related to the much smaller (or even absent) pseudogap energy scale with respect to hole-doped materials.[8,29]

ACKNOWLEDGMENTS

We thank S. A. Kivelson for enlightening comments, in particular, for pointing out the correct interpretation of the finite-size scaling of $\Delta\mu$. This work was supported by the Deutsche Forschungsgemeinschaft within the Forschergruppe FOR538 and, partially, by the Austrian Science Fund (FWF Projects No. P18505-N16 and No. P18551-N16), as well as by the KONWIHR supercomputing network in Bavaria.

[1] P. W. Anderson, Science **235**, 1196 (1987).
[2] T. A. Maier, M. Jarrell, T. Pruschke, and M. H. Hettler, Rev. Mod. Phys. **77**, 1027 (2005).
[3] M. H. Hettler, A. N. Tahvildar-Zadeh, M. Jarrell, T. Pruschke, and H. R. Krishnamurthy, Phys. Rev. B **58**, R7475 (1998).
[4] G. Kotliar, S. Y. Savrasov, G. Pálsson, and G. Biroli, Phys. Rev. Lett. **87**, 186401 (2001).
[5] A. I. Lichtenstein and M. I. Katsnelson, Phys. Rev. B **62**, R9283 (2000).
[6] M. Potthoff, M. Aichhorn, and C. Dahnken, Phys. Rev. Lett. **91**, 206402 (2003).
[7] C. Dahnken, M. Aichhorn, W. Hanke, E. Arrigoni, and M. Potthoff, Phys. Rev. B **70**, 245110 (2004); C. Dahnken, M. Potthoff, E. Arrigoni, and W. Hanke, Fiz. Nizk. Temp. **32**, 602 (2006).
[8] M. Aichhorn and E. Arrigoni, Europhys. Lett. **72**, 117 (2005).
[9] M. Aichhorn, E. Arrigoni, M. Potthoff, and W. Hanke, Phys. Rev. B **74**, 024508 (2006).
[10] Notice that the maximum cluster size we can reach is smaller than in conventional Lanczos calculations. This is due to the fact that (i) we do not conserve particle numbers within the cluster in the SC phase, (ii) we have open boundary conditions within the cluster, and (iii) the cluster exact diagonalization has to be reiterated many times before convergence in the three variational parameters (see below) has been achieved.
[11] T. A. Maier, M. Jarrell, T. C. Schulthess, P. R. C. Kent, and J. B. White, Phys. Rev. Lett. **95**, 237001 (2005).
[12] D. Sénéchal, P.-L. Lavertu, M.-A. Marois, and A.-M. S. Tremblay, Phys. Rev. Lett. **94**, 156404 (2005).
[13] M. Capone and G. Kotliar, Phys. Rev. B **74**, 054513 (2006).
[14] T. A. Maier, M. S. Jarrell, and D. J. Scalapino, Phys. Rev. Lett. **96**, 047005 (2006).
[15] M. Potthoff, Eur. Phys. J. B **32**, 429 (2003); **36**, 335 (2003).
[16] M. Potthoff, Adv. Solid State Phys. **45**, 135 (2005).
[17] D. Sénéchal, D. Perez, and M. Pioro-Ladriere, Phys. Rev. Lett. **84**, 522 (2000).
[18] A. L. Fetter and J. D. Walecka, *Quantum Theory of Many-Particle Systems* (McGraw-Hill, New York, 1971).
[19] M. G. Zacher, R. Eder, E. Arrigoni, and W. Hanke, Phys. Rev. B **65**, 045109 (2002).
[20] Occasionally, one of the poles of $\boldsymbol{M}$ may have a vanishing residue in Eq. (10). In this case, one can show that $\boldsymbol{G}'$ has a corresponding pole at the same frequency with a vanishing residue so that the contribution to Eq. (3) from this pole cancels out exactly.
[21] The factor 2 comes from the separate calculation of the photoemission and inverse photoemission part.
[22] R. Freund, in *Templates for the Solution of Algebraic Eigenvalue Problems: A Practical Guide*, edited by Z. Bai, J. Demmel, J. Dongarra, A. Ruhe, and H. van der Vorst (SIAM, Philadelphia, 2000), Chapter 4.6.
[23] See, for example, S. A. Kivelson, I. P. Bindloss, E. Fradkin, V. Oganesyan, J. M. Tranquada, A. Kapitulnik, and C. Howald, Rev. Mod. Phys. **75**, 1201 (2003).
[24] C. S. Hellberg and E. Manousakis, Phys. Rev. Lett. **83**, 132 (1999); C. S. Hellberg and E. Manousakis, *ibid.* **78**, 4609 (1997); Phys. Rev. B **61**, 11787 (2000).
[25] S. R. White and D. J. Scalapino, Phys. Rev. Lett. **91**, 136403 (2003).
[26] F. Becca, M. Capone, and S. Sorella, Phys. Rev. B **62**, 12700 (2000).
[27] V. J. Emery and S. A. Kivelson, Physica C **209**, 597 (1993).
[28] U. Löw, V. J. Emery, K. Fabricius, and S. A. Kivelson, Phys. Rev. Lett. **72**, 1918 (1994).
[29] L. Alff, Y. Krockenberger, B. Welter, M. Schonecke, R. Gross, D. Manske, and M. Naito, Nature (London) **422**, 698 (2003).
[30] R. Preuss, W. Hanke, and W. von der Linden, Phys. Rev. Lett. **75**, 1344 (1995); R. Preuss, W. Hanke, C. Gröber, and H. G. Evertz, *ibid.* **79**, 1122 (1997).